

Microthrombi As A Major Cause of Cardiac Injury in COVID-19: A Pathologic Study

Running Title: *Pellegrini, Kawakami, Sakamoto, Kawai, et al.; Microthrombi and of Cardiac
Injury in COVID-19*

Dario Pellegrini, MD^{1*}; Rika Kawakami, MD^{2*}; Giulio Guagliumi, MD¹;
Atsushi Sakamoto, MD^{2*}; Kenji Kawai, MD^{2*}; Andrea Gianatti, MD¹; Ahmed Nasr, MD¹;
Robert Kutys, PA²; Liang Guo, PhD²; Anne Cornelissen, MD²; Lara Faggi, PhD¹;
Masayuki Mori, MD²; Yu Sato, MD²; Irene Pescetelli, MD¹; Matteo Brivio, MD¹;
Maria Romero, MD²; Renu Virmani, MD²; Alope V. Finn, MD^{2,3}



¹Ospedale Papa Giovanni XXIII Bergamo, Italy; ²CVPath Institute, Inc. Gaithersburg, MD;
³University of Maryland, Baltimore, MD

*Equal contribution

Address for Correspondence:

Alope V. Finn, MD
CVPath Institute Inc.
19 Firstfield Road, Gaithersburg, MD 20878
Email: afinn@cvpath.org

This article is published in its accepted form, it has not been copyedited and has not appeared in an issue of the journal. Preparation for inclusion in an issue of *Circulation* involves copyediting, typesetting, proofreading, and author review, which may lead to differences between this accepted version of the manuscript and the final, published version.

Abstract

Background: Cardiac injury is common in hospitalized patients with COVID-19 and portends poorer prognosis. However, the mechanism and the type of myocardial damage associated with SARS-CoV-2 remain uncertain.

Methods: We conducted a systematic pathologic analysis of 40 hearts from hospitalized patients dying of Coronavirus Disease 2019 (COVID-19) in Bergamo, Italy to determine the pathologic mechanisms of cardiac injury. We divided the hearts according to presence or absence of acute myocyte necrosis and then determined the underlying mechanisms of cardiac injury.

Results: Of the 40 hearts examined, 14 (35%) had evidence of myocyte necrosis, predominantly of the left ventricle. As compared to subjects without necrosis, subjects with necrosis tended to be female, have chronic kidney disease, and shorter symptom onset to admission. The incidence of severe coronary artery disease (i.e., >75% cross sectional narrowing) was not significantly different between those with and without necrosis. 3/14 (21.4%) subjects with myocyte necrosis showed evidence of acute myocardial infarction defined as ≥ 1 cm² area of necrosis while 11/14 (78.6%) showed evidence of focal (> 20 necrotic myocytes with an area of ≥ 0.05 mm² but <1 cm²) myocyte necrosis. Cardiac thrombi were present in 11/14 (78.6%) cases with necrosis, with 2/14 (14.2%) having epicardial coronary artery thrombi while 9/14 (64.3%) had microthrombi in myocardial capillaries, arterioles, and small muscular arteries. We compared cardiac microthrombi from COVID-19 positive autopsy cases to intramyocardial thromboemboli from COVID-19 cases as well as to aspirated thrombi obtained during primary percutaneous coronary intervention from uninfected and COVID-19 infected patients presenting with ST-segment elevation myocardial infarction (STEMI). Microthrombi had significantly greater fibrin and terminal complement C5b-9 immunostaining as compared to intramyocardial thromboemboli from COVID-19 negative subjects and to aspirated thrombi. There were no significant differences between the constituents of thrombi aspirated from COVID-19 positive and negative STEMI patients.

Conclusions: The most common pathologic cause of myocyte necrosis was microthrombi. Microthrombi were different in composition as compared to intramyocardial thromboemboli from COVID-19 negative subjects and to coronary thrombi retrieved from COVID-19 positive and negative STEMI patients. Tailored anti-thrombotic strategies may be useful to counteract the cardiac effects of COVID-19 infection.

Key Words: COVID-19; SARS-CoV-2; heart; cardiovascular disease

Non-standard Abbreviations and Acronyms:

COVID-19-Coronavirus Disease 2019

STEMI-ST-segment elevation myocardial infarction

RT-PCR- reverse transcriptase polymer chain reaction

in-situ hybridization-ISH

transmission electronic microscopy-TEM

Thrombolysis in myocardial infarction-TIMI

Left ventricle-LV

Right ventricle-RV

Clinical Perspective

What is new?

- Cardiac injury in COVID-19 infection is not uncommon yet the mechanism by which it occurs remains uncertain
- In this autopsy examination of 40 hearts from subjects dying of COVID-19 infection, 14 (35%) had evidence of myocyte necrosis, predominantly of the left ventricle
- The major cause of myocyte necrosis was microthrombi occurring in 9/14 (64%) cases which were distinct in composition (i.e. greater fibrin and c5b-9 complement) as compared to intramyocardial thromboemboli from COVID-19 negative subjects and to coronary thrombi retrieved from COVID-19 positive and negative STEMI patients

What are the clinical implications?

- Clinicians should be aware of the possibility of microthrombi which may not be detectable clinically as a cause of cardiac injury in subjects with COVID-19 infection
- The use of tailored anti-thrombotic strategies to counteract the effects of microthrombi on the heart may be useful and should be examined



Introduction

Myocardial injury is a common phenomenon in hospitalized patients with Coronavirus Disease 2019 (COVID-19) and is associated with worse outcomes. In one study in which troponin I was measured within 24 hours of admission to assess myocardial damage 36% of patients had elevated troponin I concentrations.¹ After adjusting for disease severity and relevant risk factor differences, even small amounts of myocardial injury were associated with increased risk of death.

The cause of myocardial injury in patients with COVID-19 has not been previously elucidated in a systematic manner. Various pathophysiological mechanisms have been hypothesized including direct viral invasion of the heart or immune-mediated cardiac injury causing myocarditis, stress-cardiomyopathy, myocardial supply-demand mismatch leading to type II myocardial infarction, cytokine storm and hypercoagulability resulting in either increased risk of epicardial coronary thrombosis, pulmonary emboli, and/or microvascular thrombi.² We recently reported a case of a young woman dying of ST-segment elevation myocardial infarction (STEMI) and cardiogenic shock who was found to have multiple myocardial microthrombi at autopsy but the prevalence of such finding among hospitalized patients with COVID-19 has not been reported³. Understanding the exact nature of cardiac injury in patients with COVID-19 may impact public health strategies, diagnostic testing, and new therapeutic trials for those infected with COVID-19.

Here we report the analysis of 40 cardiac autopsies conducted on hospitalized patients dying of COVID-19 during the height of the pandemic in Bergamo, Italy. Our goals were to systematically determine 1) the frequency of cardiac injury in hospitalized patients as assessed

by autopsy findings of myocyte necrosis; 2) the major causes and risk factors for myocardial injury; 3) the pathophysiology of cardiac necrosis in subjects infected with COVID-19.

Methods

The current analysis was performed in the frame of a systematic pathology study to assess cardiac injury by COVID-19 infection. The data that support the findings of this study are available from the corresponding author upon reasonable request.

The hearts of 40 unselected patients dying from COVID-19 at Ospedale Papa Giovanni XXIII, in Bergamo (Italy) and undergoing autopsy were collected and sent to CVPath institute for detailed pathological analysis (Gaithersburg, Maryland, United States). Study protocol was reviewed and approved by the ethical committee at Ospedale Papa Giovanni XXIII Bergamo (2020-0056), Italy and by the CVPath Institute IRB (RP0112), Gaithersburg, MD, US and registered at ClinicalTrials.gov identifier: NCT04367792.

All patients had a laboratory-confirmed diagnosis of SARS-CoV-2 infection either by nasal swab test upon admission (39/40 patients) or by post-mortem reverse transcriptase polymer chain reaction (RT-PCR). Demographic data, medical history, clinical presentation, treatment and in-hospital course were derived from medical records. All patients were managed according to local clinical practice.

The specimens were anonymized before shipping and the examining pathologist was blinded to the clinical details. All tissue specimens were fixed in 10% buffered formalin for at least 72-96 hours prior to shipment. Whole hearts and lungs (either paraffin blocks or tissues), were sent to CVPath Institute for pathologic examination.

Pathologic Analysis

Hearts were radiographed and coronary arteries with significant calcification were removed from the heart, radiographed, decalcified as necessary prior to dehydration and sectioned at 3 to 4 mm intervals at the time of embedding in paraffin to determine the extent of luminal narrowing.

Coronary arteries without any significant calcification were cut on the heart at 3 to 4 mm intervals and sections submitted with the maximal narrowing from the four major coronary arteries (left main, left anterior descending, left circumflex and the right coronary arteries). If no significant narrowing was observed section from the proximal 4 major coronary arteries were submitted. A total of 14 transmural sections of myocardium (anterior, inferior, and lateral left ventricle [LV], ventricular septum, anterior and inferior wall of the right ventricle [RV] at mid and apex, and one each from the left and right atrium) were dehydrated, embedded in paraffin, and sectioned at 4-6 μ m intervals, stained with hematoxylin and eosin (H&E), and Masson's trichrome stain for histologic evaluation. Acute myocardial infarction was defined as areas of myocyte necrosis ≥ 1 cm² whereas focal myocyte necrosis was defined as necrosis of >20 myocytes with an area of necrosis ≥ 0.05 mm² but < 1 cm² (Figure 1).

Additional sections from the slides with areas of interest were cut and stained by immunoperoxidase stains with anti-CD61 (prediluted, 760-4247, Ventana Medical Systems, Inc., AZ, USA), anti-vWF (dilution 1:4000, A0082, Agilent Technologies, CA, USA), anti-fibrin II(dilution 1:100, NYBT2G1, Accurate Chemicals, Westbury, NY, USA), anti-D-dimer(dilution 1:100, NBP1-05045, Novus Biologicals), and anti-complement C5b-9 (dilution 1:800, ab66768, abcam, Cambridge, MA, USA). Area of percent positive staining was quantified by ZEN (Zeiss) or HALO software (Indica labs) as previously described.⁴

Total RNA was extracted from myocardial tissue and coronary artery samples. Concentration and quality of RNA samples were measured. Quantitative RT-PCR was performed using specifically designed primers for SARS-CoV-2 (N1 and N2 from CDC EUA assay, Integrated DNA Technologies [IDT], Coralville, IA, USA). RNase P was used as a control and all RNA samples from the lung and heart had a cycle threshold (Ct) \leq 40. The detection of SARS-CoV-2 RNA was determined by the amplification at Ct \leq 40.⁵

To detect SARS-CoV-2 within formalin-fixed paraffin embedded tissue sections, RNA scope in-situ hybridization (ISH, Advanced Cell Diagnostics, Hayward, CA, USA) was visualized by confocal microscopy (LSM800, Zeiss, Oberkochen, Germany). SARS-CoV-2 viral RNA positive cells were visualized by the colocalization of SARS-CoV-2 positive-sense (genomic; violet) and negative-sense (replicative intermediate; turquoise) probes. 

Immunofluorescence staining for CD61/CD42b and VE-cadherin were performed using the same or adjacent sections as ISH.

For transmission electronic microscopy (TEM), heart samples were fixed with 2.5% glutaraldehyde in 0.1M sodium phosphate buffer at 4 degrees and then 1% osmium tetroxide was used for post fixation. Tissues were dehydrated by graded alcohol and embedded in EPON Resin. Ultrathin sections were cut at 80 nm with a microtome. Specimens were assessed with the TEM (Hitachi H-7650, Hitachi Science Systems Ltd., Japan).

Analysis of Coronary Artery Aspirates

A comparative analysis of the constituents of thrombus was performed between microthrombi derived from autopsy cases from subjects with COVID-19 (n=5), intramyocardial thromboemboli from COVID-19 negative subjects (n=5) obtained at random from the CVPPath Sudden Cardiac Death Registry and thrombus aspirates retrieved from the culprit lesion of

coronary arteries in COVID-19 positive and COVID-19 negative STEMI cases (5 of each) presenting with STEMI, and undergoing primary percutaneous coronary intervention in the same time span of the pathology data collection. Manual thrombus aspiration was performed according to clinical practice (indication and procedure). Patients with an occluded culprit coronary artery Thrombolysis in myocardial infarction (TIMI) flow rate 0-1 at baseline coronary angiography or patients with an open artery (TIMI 2-3) but with large filling defect or haziness in a segment reachable by a thrombectomy catheter, were selected for the study. Aspirates were fixed in 10% formalin and shipped to CVPath for analysis. This protocol was reviewed and approved by the ethical committee at Ospedale Papa Giovanni XXIII Bergamo, Italy (2020-082) and by the CVPath Institute IRB, Gaithersburg, MD, US (RP0112). Aspirates were embedded in paraffin, cut, and stained with the indicated antibodies as described above.



Statistical Analysis

Normality of data was checked using Shapiro-Wilk test. For normally distributed data, ANOVA or student's t-test was used to compare data. For multiple comparisons testing, Tukey-Kramer post-hoc testing was used. Categorical values were analyzed by the Chi-Square or Fisher's exact test as appropriate. For non-normally distributed data, the Wilcoxon rank sum test and post-hoc Steel-Dwass tests were applied. A p value <0.05 was considered significant. JMP (version 14, SAS, Cary, NC, USA) or GraphPad Prism (GraphPad Software version 8.2.1, La Jolla, CA, USA) software was used for statistical analysis as appropriate.

Results

Clinical characteristics of the 40 autopsy cases examined are shown in Table 1. Average age was 74 with the majority of patients (29/40, 72.5%) being male. Most (90%) were admitted for severe

respiratory failure (median PaO₂/FiO₂ [P/F] Ratio 123) while four patients (10%) presented with a cardiovascular emergency (three STEMI, one stroke). Except for the patients admitted with STEMI, no other cases of clinical myocardial infarction were recorded during hospitalization. However, 20% of EKGs in the overall study group showed abnormalities suggestive of ischemia (i.e. ST segment elevation/depression > 0.1 mV, new left bundle branch block, or inverted T wave), although not associated with chest pain.

Hearts were examined blindly at CVPPath Institute without knowledge of the clinical finding except that all subjects had died of COVID-19 (as confirmed by laboratory testing during hospitalization). Analysis revealed the presence of myocyte necrosis in 14 out of the 40 (35%) cases. Three of these 14 cases (21.4%) had evidence of acute myocardial infarction defined as an area of necrosis ≥ 1 cm², while 11 (78.6%) had focal myocyte necrosis (i.e. ≥ 0.05 mm² but <1 cm² contiguous area). There was no difference in the presence of severe coronary artery disease (defined as epicardial coronary stenosis >75% cross sectional area narrowing) between cases with and without myocardial necrosis. Details of the pathologic findings of the heart and lungs are shown in Table 2. Overall, heart weight, LV cavity size and LV and RV wall thickness were not significantly different between those with and without myocardial necrosis (Supplemental Figure I). Similarly, lung pathology such as diffuse alveolar damage, pulmonary artery thrombi or microthrombi in alveolar septa were not different between cases with and without necrosis (Table 2). None of the hearts examined had evidence of myocarditis as defined by the European Society of Cardiology.⁶ Other significant cardiovascular findings such as the presence of amyloid, hypertensive heart disease (i.e. hypertrophy) and valvular disease are listed in Table 2.

Once the pathologic findings were characterized, the clinical and laboratory findings were unblinded and divided according to the presence and absence of myocardial necrosis as shown in Tables 1 and 3. Overall, subjects with necrosis were more frequently female as compared to the patients without necrosis (50% versus 84.6%, $p=0.03$), had a greater prevalence of chronic kidney disease (35.7% vs 7.7%, $p=0.04$), a higher rate of STEMI at presentation (21.4% vs 0%, $p=0.04$), and a shorter interval between symptom onset and hospital admission (4.0 vs 6.5 days, $p=0.02$). Subjects with myocardial necrosis had lower values of hemoglobin and C-reactive protein (CRP), and greater high-sensitivity Troponin I values (23,386 vs 226, $p=0.03$) and a higher rate of ischemic EKG changes (42.9% vs 8.3%, $p=0.03$; Table 3). No difference in the degree of respiratory impairment was detected, as confirmed by the similar values of P/F ratio and similar degrees of ventilatory support. In-hospital therapy and rate of adverse events were also similar between the subjects with versus without myocardial necrosis (Supplemental Table I). Molecular analysis of RNA extracted from the lungs and various areas of the heart revealed the presence of virus in the lungs as detected by PCR in most of the 40 cases (34 out of 40 [85%]), but it was detectable in the heart in only 8 cases (20%) (Supplemental Table II). There was no difference in virus presence in cases of necrosis versus no necrosis.

Table 4 lists the pathological findings in the 14 subjects with myocyte necrosis. Two cases had evidence of epicardial coronary thrombosis in the setting of severe coronary atherosclerosis and underwent percutaneous coronary intervention. 4/14 (28.6%) cases had evidence of right ventricular (RV) strain as indicated by RV necrosis (Table 4). Of the 11 cases with focal myocyte necrosis 8 (72.7%) had microthrombi while 3 (27.3%) showed no microthrombi. Microthrombi were observed in 9 of 14 (64.3%) cases with myocyte necrosis, 8

with focal necrosis and one with acute myocardial infarction. We measured the distribution and extent of focal myocyte necrosis and microvessel thrombosis in COVID-19 subjects. Overall, focal myocardial necrosis was more common in the left ventricular inferior and lateral wall and ventricular septum as follows (inferior 55%, lateral 36%, septum 36%, inferior RV 36%, anterior LV 18%, atria 9%, and anterior RV 0%) (Supplemental Figure II). The distribution pattern of microthrombi were similar to focal myocyte necrosis (inferior LV 67%, lateral LV 56%, ventricular septum 44%, inferior RV 44%, anterior LV 22%, anterior RV 11%, and atria 11%) (Supplemental Figure II). Focal necrosis was found in 13% of histology sections (22/154 sections from 11 patients). Similarly microthrombi were observed in 27.7% of histology sections (31/126 sections from 9 patients). The presence of microthrombi was significantly associated with the presence of focal necrosis in a section-based analysis ($p < 0.01$, Fisher's Exact test, Supplemental Figure III). A cumulative distribution curve showing the % area of microthrombi per 1 mm² myocardial tissue is shown in Supplemental Figure IV. Only one case of microthrombi was associated with acute myocardial infarction. In this case the subject presented with STEMI involving the inferior and lateral regions of the left ventricle and poster wall of the right ventricle accompanied by profound cardiogenic shock causing global myocyte necrosis as described previously.³ Coronary artery disease was generally mild to moderate in almost all cases of microthrombi. None of the cases with myocyte necrosis had an unstable coronary plaque phenotype.

Because recent reports have suggested SARS-CoV-2 may be found within endothelial cells in the hearts of subjects dying of COVID-19, we conducted ISH and indirect immunofluorescence as well as TEM to look for virus presence in COVID-19 hearts with evidence of microthrombi. In the 3 hearts examined by ISH, rare virus presence could be found

in cardiac myocytes (without associated inflammation) but not in microvascular endothelial cells with evidence of microthrombi (Figure 2). Similarly, by TEM no evidence of virus particles could be found within endothelial cells in vessels with and without microthrombi in the 5 hearts examined (Figure 2). These data suggest direct endothelial infection is likely not a major mechanism of cardiac microthrombi formation in subjects with COVID-19 infection.

We compared the constituents of thrombi between coronary thrombus aspirates retrieved from the culprit lesions of a separate group of COVID-19 positive and COVID-19 negative STEMI cases (5 of each) treated during the height of the pandemic to 5 of the autopsy cases with myocardial microthrombi already described and to 5 additional cases from COVID-19 negative patients with evidence of intramyocardial thromboemboli (associated with epicardial coronary thrombosis in all cases) from the CVPPath Sudden Coronary Death Registry. Clinical  characteristics of the four groups are shown in Supplemental Table III. Given the previous connection between COVID-19 and hypercoagulability, we examined factors known to be involved with clotting using antibodies against platelets (CD61), Fibrin-II, von Willebrand Factor (vWF), D-dimer, and terminal complement complex C5b-9 also known as the membrane attack complex (MAC). Microthrombi from COVID-19 subjects were richer in Fibrin-II as compared to both myocardial thromboemboli from COVID-19 negative autopsies as well as to aspirates from STEMI patients (both non COVID-19 and COVID-19) (Fibrin-II % area: microthrombi from COVID-19 positive subjects 71.8[57.4-85.1], non-COVID-19 thromboemboli 35.6[10.1-58.7], non-COVID-19 STEMI thrombus aspirates 21.3[12.3-24.0], COVID-19 STEMI thrombus aspirates 36.7[12.4-52.1], overall $p < 0.0001$). Microthrombi from COVID-19 positive subjects were also richer in C5b-9 compared to non-COVID-19 myocardial thromboemboli and to COVID-19 negative and COVID-19 positive STEMI thrombus aspirates (C5b-9 % area:

microthrombi from COVID-19 positive subjects 19.3[6.7-39.2], non-COVID-19 thromboemboli 0.001[0-0.047], non-COVID-19 STEMI thrombus aspirates 0.22[0.036-0.28], and COVID-19 STEMI thrombus aspirates 0.027[0.014-8.5], overall $p < 0.0001$) (Figure 3). However, thromboemboli associated with epicardial coronary thrombosis from COVID-19 negative cases had significantly greater percent area of CD61 (platelet) staining (overall $p = 0.0002$) as compared to the three other groups of COVID positive and negative thrombus aspirated from patients with STEMI and COVID positive microthrombi. Constituents of thrombi aspirated from COVID-19 and non-COVID-19 STEMI patients were numerically similar.

Discussion

COVID-19 infection continues to be a major cause of mortality throughout the world. Evidence of cardiac injury as indicated by elevated levels of cardiac troponin is not uncommon in hospitalized patients and increases risk of death. In one case series from New York involving 18 patients with confirmed diagnosis of COVID-19 and ST-segment elevation, 44% received a diagnosis of acute coronary thrombosis causing myocardial infarction while 56% had evidence of non-coronary myocardial injury (defined as nonobstructive disease on coronary angiography).⁷ Of the patients with non-coronary myocardial injury 90% died, suggesting a desperate need for better understanding its pathogenesis and how best to treat them. Here we report the first systematic analysis of the causes of cardiac injury in subjects dying of COVID-19 infection. In our series, 35% of subjects had evidence of cardiac injury as indicated by myocardial necrosis at autopsy. The most common cause of necrosis was microthrombi found in 64% of cases with myocyte necrosis. Microthrombi were distinctly different in composition as

compared to epicardial coronary thrombus aspirates from STEMI cases, consisting of higher levels of fibrin and terminal complement.

While many studies have focused on pulmonary findings of COVID-19, few pathology studies have been conducted specifically examining the effects of COVID-19 on the heart and most of these did not describe specific findings related to myocardial injury. In the largest series of autopsies conducted in a New York hospital, hearts from 25 cases were evaluated. Most hearts showed evidence of pre-existing atherosclerotic or hypertensive heart disease with 60% of cases showing non-specific patchy mild interstitial chronic inflammation within the myocardium without associated myonecrosis.⁸ More recently Basso C et al. reported the findings from 21 autopsy case collected from four hospitals around the world and reported a 14.2% (3/21 cases) incidence of myocarditis.⁹ Other pathologic series have documented rare findings of lymphocytic myocarditis without clear clinical sequelae while clinical case reports have described myocardial injury presumed to be consistent with myocarditis but without actual tissue diagnosis.^{10, 11} Indeed, after quantification of viral load in 39 consecutive autopsy cases from Germany SARS-CoV-2 could be documented in 24 of 39 (61.5%) with 26 of 39 (41%) having copy numbers higher than 1000 copies per ug RNA.¹² There was no difference in inflammatory infiltrate or leukocyte numbers between individuals with and without cardiac infection. We were able to recover viral RNA in only 20% of hearts studied despite it being detectable in lungs in the vast majority of cases (85%). Indeed, in our series there were no differences in the percentage of cases with viral RNA detected in the heart with and without myocardial necrosis (14.3% vs. 23.1%, $p=0.51$), suggesting direct viral invasion of the heart does not play a major role in the development of necrosis.



While direct infection of the lungs with resulting multifocal pneumonia is thought to be the major cause of death in COVID-19 victims, inflammatory cytokine syndrome may also be an important cause of morbidity and mortality. Li et al reported significantly increased levels of IL-8, IL-6, TNF-alpha, MCP-1 and RANTES in severe COVID-19 cases and IL-6 and 8 were associated with disease progression.¹³ It is thought that severely ill COVID-19 patients are at an increased risk for thromboembolic events including pulmonary microthrombi as well as venous thrombosis perhaps resulting from cytokine storm. We show presence of microthrombi in the hearts of COVID-19 related deaths as the leading cause of cardiac injury. An autopsy case series of 32 cases from New York reported 77% had elevated troponin I. Pathologically, one case showed epicardial coronary artery thrombi and 19% had intramyocardial small vessel thrombi.¹⁴ Furthermore, Bois et al. found non-occlusive microthrombi in the small intramyocardial vasculature in 80% (12/15) of COVID-19 autopsy cases.¹⁵ Of note, they reported only 2 out of 15 patients (13.3%) had acute ischemic injury. A multicenter autopsy study by Basso et al. reported acute myocyte injury in the right ventricle and thrombi in small vessels of myocardium in 4 out of 21 cases (19% in both cases).⁹ However, their distribution and association with necrosis were not described. We had previously reported one case of microthrombi in a COVID-19 infected young female patient who died of acute myocardial infarction and cardiogenic shock but now we have expanded our findings in a larger series of cases (n=40) and found that microthrombi are the leading cause of cardiac injury (defined as myocyte necrosis). Rapkiewicz also reported autopsy findings of 7 cases with COVID-19 with 5 of the 7 being hospitalized at the time of death and 2 suffering sudden cardiac death at home.¹⁶ In all 7 cases fibrin microthrombi were identified in the heart, however, the extent of microthrombi and their location was not specifically identified nor was the extent of myocardial necrosis. Although staining for



complement (C4d) was performed to rule out complement-mediated myocyte damage, and was negative in all cases tested, complement in microthrombi was not specifically examined.

Cardiac microthrombi would not be detectable clinically as no laboratory test can specifically detect microthrombi but future studies should be directed towards developing methods and laboratory testing to diagnose this type of injury. Overall, there was a significant difference in ischemic EKG changes in those with versus without myocyte necrosis although sensitivity of such findings was poor as only 6 of the 14 (42.9%) cases showed myocardial injury by EKG. Clinical presentation may also be misleading, as chest pain may be absent or significantly under-reported, especially in patients suffering from severe respiratory impairment.

We found that microthrombi were distinct in composition as compared to epicardial thrombus aspirates from STEMI patients with and without COVID-19 infection with higher levels of fibrin and terminal complement. A recent study of SARS-CoV, which is closely related to SARS-CoV-2 found disease exacerbation was related to the activation of complement C3.¹⁷ Others have reported that SARS-CoV-2 autoactivates mannan-binding lectin-associated serine protease 2 (MASP-2), the primary enzymatic initiator of the lectin pathway.¹⁸ MASP-2 activation leads to generation of C3 convertase and activation of the MAC (C5b-9).¹⁹ Moreover, alteration of the MASP-2-binding motif, either by *Masp2* deletion or blocking the MASP-2-N protein interaction, attenuated lung injury.¹⁸ Immunohistochemistry analysis of pulmonary autopsy samples revealed MASP2 and C5b-9 deposition localized in interalveolar septa. These data, along with human proteomic studies suggest that coronavirus infections are associated with the activation of multiple complement pathways.²⁰⁻²²

Moreover, inhibiting complement pathway seems to have a therapeutic effect at least in experimental models.^{17, 21} C3 deficient mice infected with SARS-CoV exhibited less respiratory problems despite similar viral loads in the lung with lower levels of cytokines found in the lung and serum.¹⁷ The reduction in lung neutrophils reduced intrapulmonary and plasma IL-6 levels. Currently, C3 blockade with agents such as AMY-101 are undergoing clinical trials in patients infected with COVID-19 (NCT04395456).

We should also address some of the limitations of this study. Autopsy material from subjects dying of COVID-19 infection may have its own biases and may not be reflective of cardiac findings in those who survive COVID-19 infection. Thus, the true incidence of cardiac injury and microthrombi may be different in subjects who survive COVID-19 infection. Moreover, the lack of troponin levels in all subjects also may limit the clinical translation of myocardial necrosis detected at autopsy. Although we surveyed all regions of the heart at multiple levels, small areas of necrosis and microthrombi may have been missed, because of sampling. Nonetheless, we believe this study reveals important and novel insights about the nature of cardiac injury in subjects dying of COVID-19 infection.

In conclusion, our study is the first to examine systematically the causes of cardiac injury in patients dying of COVID-19 infection. Here we report that 35% of subjects dying with COVID-19 had evidence of cardiac injury as identified by the presence of myocyte necrosis with the majority (78.6%) having focal myocyte necrosis. The major cause of myocyte necrosis was cardiac microthrombi occurring in 64.3% of those with myocyte necrosis. Microthrombi were different in thrombus constituents with richer fibrin and complement as compared to intramyocardial thrombi from COVID-negative subjects and from thrombi aspirated from coronary arteries of both COVID-19 positive and negative STEMI cases. Our data suggest that

microvascular thrombosis should be entertained as a likely cause of cardiac injury in hospitalized patients with COVID-19 and that further investigation of anti-platelet, anti-coagulant, and anti-complement therapies which specifically target microthrombi should be examined in clinical trials.

Sources of Funding

The study was funded by CVPPath Institute, a 501(c)(3) organization.

Disclosures

CVPPath Institute has received institutional research support from R01 HL141425 Leducq Foundation Grant; 480 Biomedical; 4C Medical; 4Tech; Abbott; Accumedical; Amgen; Biosensors; Boston Scientific; Cardiac Implants; Celonova; Claret Medical; Concept Medical; Cook; CSI; DuNing, Inc; Edwards LifeSciences; Emboline; Endotronix; Envision Scientific; Lutonix/Bard; Gateway; Lifetech; Limflo; MedAlliance; Medtronic; Mercator; Merill; Microport Medical; Microvention; Mitraalign; Mitra assist; NAMSA; Nanova; Neovasc; NIPRO; Novogate; Occulotech; OrbusNeich Medical; Phenox; Profusa; Protembis; Qool; Recor; Senseonics; Shockwave; Sinomed; Spectranetics; Surmodics; Symic; Vesper; W.L. Gore; Xeltis. A.V.F. has received honoraria from Abbott Vascular; Biosensors; Boston Scientific; Celonova; Cook Medical; CSI; Lutonix Bard; Sinomed; Terumo Corporation; and is a consultant to Amgen; Abbott Vascular; Boston Scientific; Celonova; Cook Medical; Lutonix Bard; Sinomed. Anne Cornelissen receives research grants from University Hospital RWTH Aachen. R.V. has received honoraria from Abbott Vascular; Biosensors; Boston Scientific; Celonova; Cook Medical; Cordis; CSI; Lutonix Bard; Medtronic; OrbusNeich Medical; CeloNova; SINO Medical

Technology; ReCore; Terumo Corporation; W. L. Gore; Spectranetics; and is a consultant Abbott Vascular; Boston Scientific; Celonova; Cook Medical; Cordis; CSI; Edwards Lifescience; Lutonix Bard; Medtronic; OrbusNeich Medical; ReCore; Sinomedical Technology; Spectranetics; Surmodics; Terumo Corporation; W. L. Gore; Xeltis. The other authors declare no competing interests.

Supplemental Materials:

Supplemental Figures I-IV

Supplemental Tables I-III

References



1. Lala A, Johnson KW, Januzzi JL, Russak AJ, Paranjpe I, Richter F, Zhao S, Somani S, Van Vleck T, Vaid A et al. Prevalence and Impact of Myocardial Injury in Patients Hospitalized With COVID-19 Infection. *J Am Coll Cardiol*. 2020;76:533-546.
2. Hendren NS, Drazner MH, Bozkurt B and Cooper LT, Jr. Description and Proposed Management of the Acute COVID-19 Cardiovascular Syndrome. *Circulation*. 2020;141:1903-1914.
3. Guagliumi G, Sonzogni A, Pescetelli I, Pellegrini D and Finn AV. Microthrombi and ST-Segment-Elevation Myocardial Infarction in COVID-19. *Circulation*. 2020;142:804-809.
4. Torii S, Jinnouchi H, Sakamoto A, Romero ME, Kolodgie FD, Virmani R and Finn AV. Comparison of Biologic Effect and Particulate Embolization after Femoral Artery Treatment with Three Drug-Coated Balloons in Healthy Swine Model. *J Vasc Interv Radiol*. 2019;30:103-109.
5. Ramlall V, Thangaraj PM, Meydan C, Foon J, Butler D, Kim J, May B, De Freitas JK, Glicksberg BS, Mason CE, et al. Immune complement and coagulation dysfunction in adverse outcomes of SARS-CoV-2 infection. *Nat Med*. 2020;26:1609-1615.
6. Caforio AL, Pankuweit S, Arbustini E, Basso C, Gimeno-Blanes J, Felix SB, Fu M, Helio T, Heymans S, Jahns R et al. Current state of knowledge on aetiology, diagnosis, management, and therapy of myocarditis: a position statement of the European Society of Cardiology Working Group on Myocardial and Pericardial Diseases. *Eur Heart J*. 2013;34:2636-48, 2648a-2648d.
7. Bangalore S, Sharma A, Slotwiner A, Yatskar L, Harari R, Shah B, Ibrahim H, Friedman GH et al. ST-Segment Elevation in Patients with Covid-19 - A Case Series. *N Engl J Med*. 2020; 382: 2478-80.
8. Bryce C, Grimes Z, Pujadas E, Ahuja S, Beasley MB, Albrecht R, Hernandez T, Stock A, Zhao Z, Al Rasheed M, et al. Pathophysiology of SARS-CoV-2: targeting of endothelial cells

- renders a complex disease with thrombotic microangiopathy and aberrant immune response. The Mount Sinai COVID-19 autopsy experience. *medRxiv*. 2020 May 22 [E-pub ahead of print].
9. Basso C, Leone O, Rizzo S, De Gaspari M, van der Wal AC, Aubry MC, Bois MC, Lin PT, Maleszewski JJ and Stone JR. Pathological features of COVID-19-associated myocardial injury: a multicentre cardiovascular pathology study. *Eur Heart J*. 2020; 41:3827-35.
 10. Schaller T, Hirschbuhl K, Burkhardt K, Braun G, Trepel M, Markl B and Claus R. Postmortem Examination of Patients With COVID-19. *JAMA*. 2020;323:2518-2520.
 11. Schurink B, Roos E, Radonic T, Barbe E, Bouman CSC, de Boer HH, de Bree GJ, Bulle EB, Aronica EM, Florquin S, Fronczek J, et al. Viral presence and immunopathology in patients with lethal COVID-19: a prospective autopsy cohort study. *Lancet Microbe*. 2020;1:e290-e299.
 12. Lindner D, Fitzek A, Brauninger H, Aleshcheva G, Edler C, Meissner K, Scherschel K, Kirchhof P, Escher F, Schultheiss HP, et al.. Association of Cardiac Infection With SARS-CoV-2 in Confirmed COVID-19 Autopsy Cases. *JAMA Cardiol*. 2020;5:1281-1285.
 13. Li S, Jiang L, Li X, Lin F, Wang Y, Li B, Jiang T, An W, Liu S, Liu H, et al. Clinical and pathological investigation of patients with severe COVID-19. *JCI Insight*. 2020;5: e138070.
 14. Elsoukkary SS, Mostyka M, Dillard A, Berman DR, Ma LX, Chadburn A, Yantiss RK, Jessurun J, Seshan SV, Borczuk AC, et al. Autopsy Findings in 32 Patients with COVID-19: A Single-Institution Experience. *Pathobiology*. 2020:1-13.
 15. Bois MC, Boire NA, Layman AJ, Aubry MC, Alexander MP, Roden AC, Hagen CE, Quinton RA, Larsen C, Erben Y, et al. COVID-19-associated Non-Occlusive Fibrin Microthrombi in the Heart. *Circulation*. 2020 Nov 16 [E-pub ahead of print].
 16. Rapkiewicz AV, Mai X, Carsons SE, Pittaluga S, Kleiner DE, Berger JS, Thomas S, Adler NM, Charytan DM, Gasmi B, et al. Megakaryocytes and platelet-fibrin thrombi characterize multi-organ thrombosis at autopsy in COVID-19: A case series. *EClinicalMedicine*. 2020;24:100434.
 17. Gralinski LE, Sheahan TP, Morrison TE, Menachery VD, Jensen K, Leist SR, Whitmore A, Heise MT and Baric RS. Complement Activation Contributes to Severe Acute Respiratory Syndrome Coronavirus Pathogenesis. *mBio*. 2018;9: 01753-18.
 18. Gao T, Hu M, Zhang X, Li H, Zhu L, Liu H, Dong Q, Zhang Z, Wang Z, Hu Y, et al. Highly pathogenic coronavirus N protein aggravates lung injury by MASP-2-mediated complement over-activation. *medRxiv*. 2020.
 19. Noris M, Benigni A and Remuzzi G. The case of complement activation in COVID-19 multiorgan impact. *Kidney Int*. 2020;98:314-322.
 20. Shen B, Yi X, Sun Y, Bi X, Du J, Zhang C, Quan S, Zhang F, Sun R, Qian L, et al. Proteomic and Metabolomic Characterization of COVID-19 Patient Sera. *Cell*. 2020;182:59-72 e15.
 21. Carvelli J, Demaria O, Vely F, Batista L, Chouaki Benmansour N, Fares J, Carpentier S, Thibult ML, Morel A, Remark R, et al. Association of COVID-19 inflammation with activation of the C5a-C5aR1 axis. *Nature*. 2020;588:146-150.
 22. Polycarpou A, Howard M, Farrar CA, Greenlaw R, Fanelli G, Wallis R, Klavinskis LS and Sacks S. Rationale for targeting complement in COVID-19. *EMBO Mol Med*. 2020;12:e12642.

Table 1. Overall Clinical Characteristics of the 40 Autopsy Cases and According to Presence or Absence of Myocardial Necrosis.

Clinical Characteristics	Total (n = 40)	Myocardial necrosis (n = 14)	No necrosis (n = 26)	P value
Age	74.00 [65.00-81.00]	74.50 [69.00-81.25]	73.50 [61.25-81.00]	0.43
Male sex	29 (72.5%)	7 (50.0%)	22 (84.6%)	0.03
Body Mass Index (BMI)	27.78 [24.72-29.32]	25.14 [23.11-32.88]	27.83 [25.28-29.50]	0.46
Hypertension	29 (72.5%)	10 (71.4%)	19 (73.1%)	1.00
Dyslipidemia	10 (25.0%)	3 (21.4%)	7 (26.9%)	1.00
Diabetes	11 (27.5%)	4 (28.6%)	7 (26.9%)	0.70
Known history of coronary artery disease	8 (20.0%)	3 (21.4%)	5 (19.2%)	1.00
Previous myocardial infarction	3 (7.5%)	1 (7.1%)	2 (7.7%)	1.00
Peripheral artery disease	6 (15.0%)	1 (7.1%)	5 (19.2%)	0.40
Valvular heart disease	1 (2.5%)	1 (7.1%)	0 (0%)	0.35
Chronic obstructive pulmonary disease	3 (7.5%)	0 (0.0%)	3 (11.5%)	0.54
Chronic kidney disease	7 (17.5%)	5 (35.7%)	2 (7.7%)	0.04
Autoimmune disorder	3 (7.5%)	0 (0.0%)	3 (11.5%)	0.54
Immunosuppression state	8 (20.0%)	5 (35.7%)	3 (11.5%)	0.10
• Active leukemia/lymphoma	5 (12.5%)	3 (21.4%)	2 (7.7%)	0.32
• Previous transplantation	3 (7.5%)	2 (14.3%)	1 (3.9%)	0.28
Therapy at home				
Acetylsalicylic acid (ASA)	18 (45.0%)	6 (42.9%)	12 (46.2%)	1.00
ACE-inhibitors	10 (25.0%)	4 (28.6%)	6 (23.1%)	0.72
Angiotensin receptor blockers (ARBs)	3 (7.5%)	0 (0.0%)	3 (11.5%)	0.54
Statin	8 (20.0%)	2 (14.3%)	6 (23.1%)	0.69
Chronic oral anticoagulant (OAC)	3 (7.5%)	2 (14.3%)	1 (3.9%)	0.28
Recent history				
Cause of admission				0.04
• Respiratory failure	36 (90.0%)	11 (78.6%)	25 (96.2%)	-
• STEMI	3 (7.5%)	3 (21.4%)	0 (0.0%)	-
• Stroke	1 (2.5%)	0 (0.0%)	1 (3.9%)	-
Interval symptom onset - admission (days)	5.00 [4.00-10.00]	4.00 [0.50-6.00]	6.50 [4.00-10.00]	0.02

Categorical variables were shown as numbers and percentages. Continuous variables were expressed as median and interquartile range.

Abbreviations; ACE: angiotensin converting enzyme, STEMI: ST-segment elevation myocardial infarction

Table 2. Pathological Findings of the Heart and Lung in Subjects With and Without Myocardial Necrosis.

	Total (n = 40)	Myocardial necrosis (n = 14)	No necrosis (n = 26)	P value
Myocardial necrosis				
Acute myocardial infarction ($\geq 1 \text{ cm}^2$)	3 (7.5%)	3 (21.4%)	0 (0%)	0.014
Focal myocyte necrosis ($\geq 0.05 \text{ mm}^2$ but $< 1 \text{ cm}^2$)	11 (27.5%)	11 (78.6%)	0 (0%)	<0.001
Thrombus				
Epicardial coronary artery thrombus	3 (7.5%)	2 (14.2%)	1 (3.8%)*	0.23
Microthrombi	9 (22.5%)	9 (64.3%)	0 (0%)	<0.001
Coronary artery disease				
Coronary stent	6 (15%)	3 (21.4%)	3 (11.5%)	0.40
Single vessel disease (>75% C-S area)	9 (22.5%)	3 (21.4%)	6 (23.1%)	0.91
Multi-vessel disease (>75% C-S area in ≥ 2 epicardial vessels)	9 (22.5%)	3 (21.4%)	6 (23.1%)	0.91
Other cardiac findings				
Myocarditis	0 (0%)	0 (0%)	0 (0%)	-
Hypertrophy of myocardium	29 (72.5%)	10 (71.4%)	19 (73.1%)	0.91
Valvular heart disease	2 (5.0%)	2 (14.3%) [†]	0 (0%)	0.21
Cardiac amyloidosis	6 (14.3%)	2 (14.3%)	4 (15.4%)	0.93
Lung Findings				
Diffuse alveolar damage	36 (92.3%)	12 (92.3%)	24 (88.9%)	0.51
Pulmonary artery thrombus	18 (46.2%)	5 (38.5%)	13 (48.1%)	0.39
Microthrombi in alveolar septa	10 (25.6%)	5 (38.5%)	5 (18.5%)	0.25

Categorical variables were shown as numbers and percentages.

*Sudden Cardiac Death.

[†] Status post-aortic valve replacement (n=1), Moderate aortic stenosis (n=1).

Abbreviations; C-S: cross sectional.

Table 3. Overall Laboratory Characteristics of the 40 Autopsy Cases and According to Presence or Absence of Myocardial Necrosis.

Lab Values	Available (n)	Total (n = 40)	Myocardial necrosis (n = 14)	No necrosis (n = 26)	P value
Hemoglobin (g/dL)	40	13.15 [11.03-14.60]	11.65 [9.70-13.55]	13.45 [11.63-15.13]	0.04
Total WBC (n/mm ³)	40	9,415 [6,128-13,063]	9,655 [6,215-12,867]	9,415 [5,990-13,557]	0.10
Neutrophil	40				
- Count (n/mm ³)		6,884 [4,275-9,713]	7,830 [5,533-11,370]	6,050 [4,145-9,427]	0.22
- Relative (%)		84.15 [70.53-89.93]	89.60 [70.88-93.05]	82.30 [69.90-86.63]	0.10
Lymphocytes	36				
- Count (n/mm ³)		725 [520-1,078]	500 [170-1,100]	750 [558-1,059]	0.19
- Relative (%)		10.10 [5.08-15.78]	4.40 [2.70-24.10]	10.20 [6.55-14.85]	0.34
Platelets (n/mm ³)	40	208,500 [136,250-292,750]	215,500 [132,500-315,750]	207,000 [134,500-255,750]	0.49
CRP (mg/dL)	40	15.45 [9.18-26.20]	11.15 [3.90-17.85]	18.90 [14.38-28.93]	0.02
Creatinine (mg/dL)	40	1.10 [0.86-1.78]	0.98 [0.75-1.82]	1.17 [0.91-1.82]	0.35
GOT (U/L)	39	47.00 [33.00-86.00]	42.00 [26.00-81.50]	53.50 [38.75-87.25]	0.23
GPT (U/L)	40	40.00 [28.25-67.50]	38.50 [20.00-80.00]	40.00 [29.75-66.50]	0.74
Tn-I (ng/L) †	15	419 [73-1,000]	23,386 [334-115,786]	226 [39-526]	0.03
D-dimer (ng/mL)	26	5,059 [1,709-16,158]	5,117 [1,418-15,471]	5,000 [1,887-17,145]	0.73
PT-INR	40	1.10 [1.04-1.18]	1.10 [1.04-1.31]	1.10 [1.02-1.17]	0.73
aPTT	40	1.12 [1.00-1.22]	1.11 [0.98-1.29]	1.12 [1.01-1.21]	0.79
IL-6 (pg/mL)	22	108.10 [68.33-210.75]	125.00 [61.05-208.50]	96.20 [66.80-265.50]	0.97
P/F ratio at presentation	36	123.00 [92.00-176.88]	112.22 [93.00-181.00]	140.0 [86.00-179.17]	0.73
Ischemic ECG changes*	38	8 (20.0%)	6 (42.9%)	2 (8.3%)	0.03
Abnormal cardiac ultrasound findings	14				
- Regional wall motion impairment		8 (57.1%)	5 (83.3%)	3 (37.5%)	0.14
- Impaired right ventricle		3 (21.4%)	3 (50.0%)	0 (0.0%)	0.05
		5 (35.7%)	2 (33.3%)	3 (37.5%)	1.00

† High-sensitivity troponin I analysis was performed based on clinical needs, according to judgement of the treating physicians. Median interval from admission to troponin evaluation was 3 days [IQR 1.5-7.5].

* Ischemic ECG changes defined as ST segment elevation/depression > 0.1 mV, new left bundle branch block, inverted T wave.

Categorical data were shown as numbers and percentages. Continuous variables were expressed as median and interquartile range.

Abbreviations; aPTT: activated partial thromboplastin time, CRP: C-reactive protein, GOT: serum glutamic oxaloacetic transaminase, GPT: serum glutamic pyruvic transaminase, IL-6: interleukin-6, PT-INR: prothrombin time international normalized ration, P/F: PaO₂/FiO₂ Tn-I: troponin I, WBC: white blood count.

Table 4. Pathological Findings of the Heart in Subjects with Myocardial Necrosis.

Case	Type of myocardial injury	Location of acute myocardial necrosis	Epicardial coronary artery acute thrombus	Coronary intervention	Epicardial CA stenosis	Healed MI	Type of thrombus in myocardium
1	AMI (Reperused, Transmural infarction)	Anterior, V Septum, Lateral, Ant RV	Yes (LAD)	Yes, LAD (stented acutely)	50% RCA, 10% LM, 70% LAD*, 70% LCX	no	PCI related intramyocardial thrombus
2	AMI (Reperused, Subendocardial infarction)	Lateral, Inferior, Anterior - LV	Yes (LCX)	Yes, LCX (In-stent restenosis and acute DCB treatment), RCA (Previous stent, open), LAD (In-stent restenosis and acute DCB treatment)	RCA 50%, 40% LM, 40% LAD, 40% LCX*	Yes	DCB (PCI) related intramyocardial thrombus
3	AMI (Focal areas of myocyte necrosis, transmural myocyte necrosis due to shock)	Circumferential	no	no	50% RCA, 50% LM, 50% LAD, 40% LCX	no	Microthrombus
4	Focal myocyte necrosis	Lateral, Inferior- LV	no	Yes, RCA(Previous stent, 30%)	80% RCA, 35% LM, 50% LAD, 50% LCX	Yes	Microthrombus
5	Focal myocyte necrosis	Inferior-LV, Inferior- RV	no	no	60% RCA, 75% LM, 75% LAD, 70% LCX	Yes	Microthrombus
6	Focal myocyte necrosis	Inferior, Anterior, Lateral-LV	no	no	65% RCA, 40% LM, 65% LAD, 50% LCX	no	Microthrombus
7	Focal myocyte necrosis	V Septum, Inferior-RV	no	no	40% RCA, 40% LM, 60% LAD, 70% LCX	no	Microthrombus
8	Focal myocyte necrosis	Inferior-LV	no	no	75% RCA, 30% LM, 65% LAD, 40% LCX	no	Microthrombus
9	Focal myocyte necrosis	V Septum	no	no	CTO RCA, 50% LM, 80% LAD, 70% LCX	no	Microthrombus
10	Focal myocyte necrosis	Lateral-LV, RA	no	no	40% RCA, 20% LM, 30% LAD, 50% LCX	no	Microthrombus
11	Focal myocyte necrosis	Anterior, V Septum Lateral, Inferior-LV	no	no	50% RCA, 20% LM, 50% LAD, 0% LCX	no	Microthrombus
12	Focal myocyte necrosis	V Septum, Inferior-RV	no	no	25% RCA, 25% LM, 25% LAD, 25% LCX	no	no
13	Focal myocyte necrosis	Inferior-RV	no	no	15% RCA, 30% LM, 30% LAD, 25% LCX	Yes	no
14	Focal myocyte necrosis	Inferior-LV	no	no	20% RCA, 5% LM, 30% LAD, 20% LCX	no	no

*Culprit vessel of acute myocardial infarction.

Abbreviations; AMI: acute myocardial infarction, CA: coronary artery, CAD: coronary artery disease, CTO: chronic total occlusion, DCB: drug-coated balloon, LAD: left anterior descending artery, LCX: left circumflex artery, LM: left main trunk, LV: left ventricle, MI: myocardial infarction, PCI: percutaneous coronary intervention, RA: right atrium, RCA: right coronary artery, RV: right ventricle, V: ventricular.

Figure Legends

Figure 1. Patterns of Myocardial Necrosis.

A, and E. Schematic illustration of myocardial necrosis patterns caused by different types of thrombi. There is a difference in the pattern of necrosis between epicardial coronary artery thrombi and microthrombi. Epicardial coronary artery thrombi are associated with confluent transmural infarction[necrosis area ($\geq 1\text{cm}^2$)] as illustrated in **A** which can be hemorrhagic when reperfused as in this case. In contrast, microthrombi cause small areas of focal necrosis (i.e., > 20 myocytes showing necrosis occupying an area $\geq 0.05\text{ mm}^2$ but $< 1\text{ cm}^2$), as illustrated in **E**.

B and F. Gross images of the transverse slice of the right and left ventricles from case 1 (**B**) and 9 (**F**) showing of acute transmural myocardial infarction in **B** and no macroscopic necrosis in **F**.

C. Histology images of myocardium stained with hematoxylin and eosin (H&E) shows typical acute transmural hemorrhagic myocardial infarction (black double arrow), which is characterized by transmural confluent areas of myocytes necrosis, hemorrhage, neutrophil infiltration, and edema.

D. High power image of the boxed area in **C** showing hemorrhage and acute inflammation in focal areas of the myocardial necrosis and edema. **G.** Histology image of focal myocardial necrosis caused by microthrombi shows smaller foci of myocardial necrosis (black circles indicate areas of focal necrosis) (Masson's trichrome stain). **H.** Black boxed area from image **G** shows an area of focal myocyte necrosis outlined by dotted black line (Masson's Trichrome stain).

Abbreviations: LV: left ventricle, RV: right ventricle.

Figure 2. ISH Fluorescence Microscopy and TEM to Detect SARS-CoV-2 in Endothelial Cells in Cases with Cardiac Microthrombi

A-C. Pathology of COVID-19 autopsy lung (80-year-old female). **A.** H&E stained section shows thickened alveolar wall with inflammatory cells, including multinuclear giant cells and the formation of hyaline membranes, consistent with exudative phase of diffuse alveolar damage. **B.** Corresponding low-power image of SARS CoV-2 RNA scope ISH. Multiple double positive cells (i.e., viral RNA positive-sense [violet] and viral RNA negative-sense [turquoise]) were observed. **C.** High-power image in white rectangle area in B shows infected alveolar pneumocyte.

D-I. Pathology of COVID-19 autopsy heart with myocardial necrosis caused by microthrombi (43-year-old female). **D.** Representative H&E images showing microthrombi (black arrows) with surrounding necrosis are observed (black dotted area). **E** Small focal lesions of myocardial necrosis were observed (black dotted area) (Masson's trichrome). **F.** Corresponding low-power image from E showing immunostaining against VE-cad (endothelial marker, green), CD61+42b (platelet marker, red), and DAPI (nuclear stain). Multiple micro vessels with platelet thrombi were observed around areas of myocyte necrosis. **G.** High-power image in white rectangular area in F shows a micro vessel with occlusive thrombus. **H.** Representative viral RNA scope image of area shown in G which is also stained against VE-cad (endothelial marker, green). No evidence of viral infection (i.e., viral RNA positive-sense [violet] and viral RNA negative-sense [turquoise]) in vascular endothelium (shown by white arrows) was observed. **I.** TEM image of cardiac microthrombus. A microvessel is filled by a fibrin-rich thrombus. There was no evidence of viral particles within endothelial cells and thrombus. **J-K.** TEM image obtained from another case of COVID-19 autopsy heart with myocardial necrosis but no microthrombi (66-year-old

male). Low- (**J**) and high-power images (**K**) failed to show any viral particles in microvascular endothelium.

Abbreviations: BM:basement membrane, cyto:cytoplasm, COVID-19:coronavirus disease-2019, DAPI: 4',6-diamidino-2-phenylindole, H&E: hematoxylin and eosin, Myo: myocyte, Nu: nucleus, RBC: red blood cell, SARS-CoV-2: severe acute respiratory syndrome coronavirus 2, TEM: transmission electron microscopy, Th: thrombus, VE-cad: vascular endothelial cadherin

Figure 3. Analysis of Thrombi Aspirated from Culprit Lesions of COVID-19 Positive and Negative STEMI Cases, Myocardial Thromboemboli from COVID-19 Negative Autopsy Subjects, and Cardiac Microthrombi from COVID-19 Positive Autopsy Subjects. A-L.

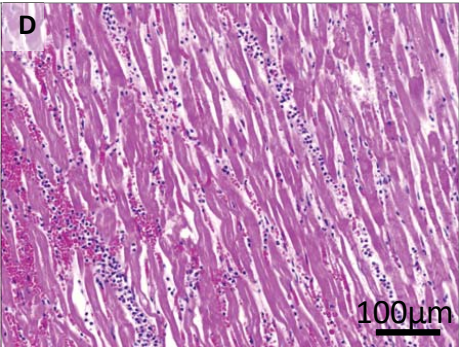
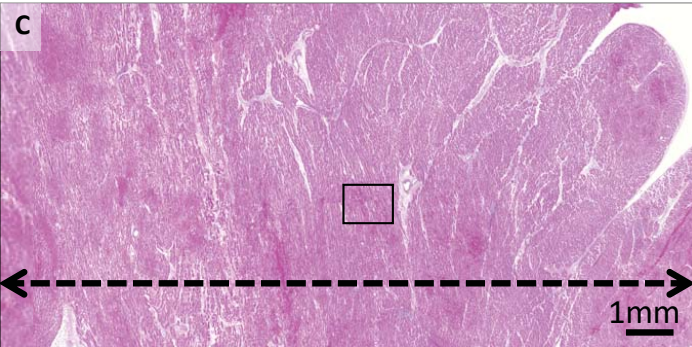
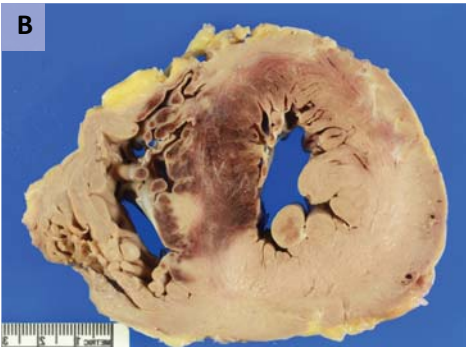
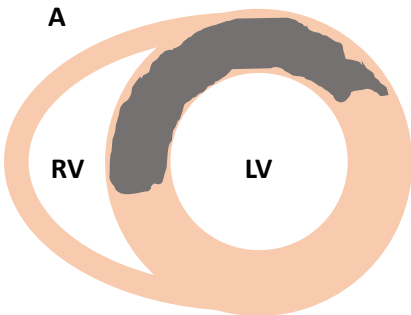
The histology images of thrombus aspirates were obtained from the same patient of non-COVID-19 (**A-F**) and COVID-19 (**G-L**) during primary PCI stained for indicated targets. Thrombus is composed primarily of platelets and fibrin but terminal complement is not present. **M-R**: The histology images of intramyocardial thromboemboli associated with epicardial coronary thrombosis from non-COVID-19 autopsy cases. **S-X**: Histology images of COVID-19 microthrombi. Microthrombi immunostaining for the same targets shows they are strongly positive for CD61, vWF, Fibrin-ll, D-dimer, and C5b-9. **Y**. Quantitative analyses of thrombus components among epicardial coronary arteries thrombus aspirates obtained from STEMI (both non-COVID-19 [n=5] and COVID-19 [n=5]) patients, intramyocardial thromboemboli associated with epicardial coronary thrombosis from non-COVID-19 autopsy cases (n=5) and microthrombus in COVID-19 autopsy cases (n=5). Overall p value for each analysis is shown (Wilcoxon Rank Sum Test); Data are expressed as median with interquartile range.

Abbreviations: C: complement, CD: cluster of differentiation, COV: COVID-19, COV-: COVID-19 negative, COV+: COVID-19 positive, COVID-19: coronavirus disease 2019, H&E: hematoxylin and eosin stain, ns: not significant, STEMI: ST-elevation myocardial infarction, vWF: von Willebrand factor.



Circulation

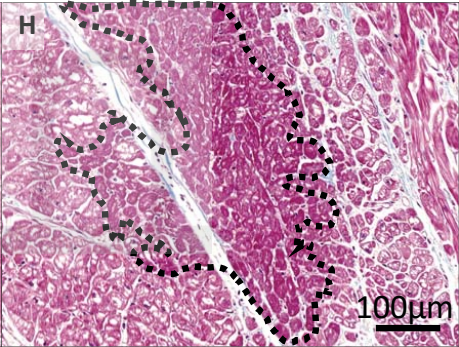
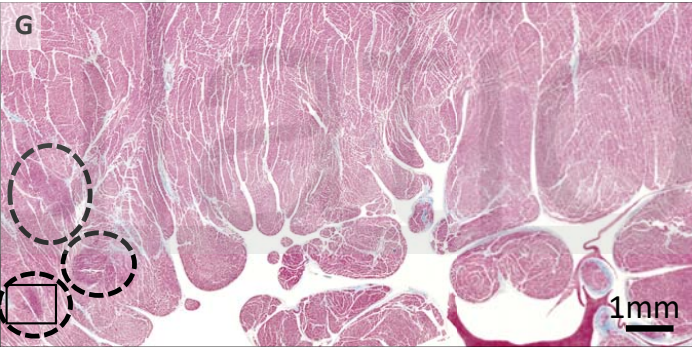
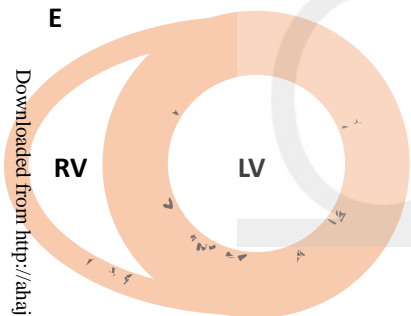
Myocardial infarction (necrosis area $\geq 1 \text{ cm}^2$)

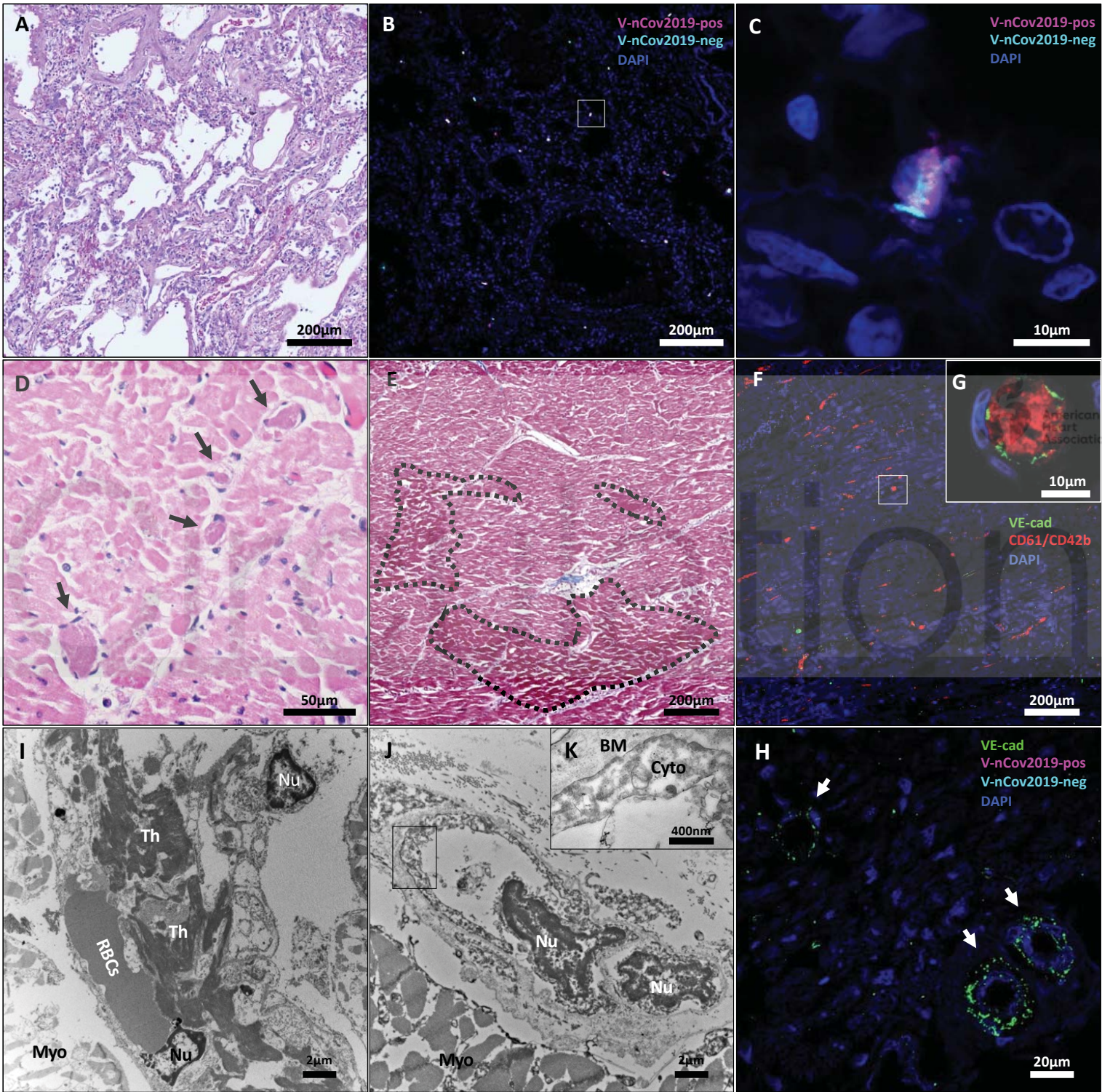


Myocardium
 Infarction/necrosis area

Focal myocyte necrosis

(> 20 myocytes showing necrosis with an area $\geq 0.05 \text{ mm}^2$ but $< 1 \text{ cm}^2$)





Coronary artery thrombus aspirates from non-COVID-19 STEMI cases

Coronary artery thrombus aspirates from COVID-19 STEMI cases

Thromboemboli associated with epicardial coronary thrombosis in non-COVID-19 autopsy cases

Microthrombi from COVID-19 autopsy cases

